Many-body approach to the nonlinear interaction of charged particles with an interacting free electron gas

2001 J. Phys. A: Math. Gen. 34 7607

(http://iopscience.iop.org/0305-4470/34/37/313)

INSTITUTE OF PHYSICS PUBLISHING JOURNAL OF PHYSICS A: MATHEMATICAL AND GENERAL

J. Phys. A: Math. Gen. **34** (2001) 7607–7620 PII: S0305-4470(01)24538-7

Many-body approach to the nonlinear interaction of charged particles with an interacting free electron gas

T del Río Gaztelurrutia[1] **and J M Pitarke**[2]

[1] Fisika Aplikatua Saila, Industri eta Telekomunikazio Ingeniarien Goi Eskola Teknikoa, Urkijo Zumarkalea z/g, S-48013 Bilbo, Basque Country, Spain
[2] Materia Kondentsatuaren Fisika Saila, Zientzi Fakultatea, Euskal Herriko Unibertsitatea, 644 Posta kutxatila, 48080 Bilbo, Basque Country, Spain and
Donostia International Physics Center (DIPC) and Centro Mixto CSIC-UPV/EHU, Donostia, Basque Country, Spain

Received 20 April 2001, in final form 3 May 2001
Published 7 September 2001
Online at stacks.iop.org/JPhysA/34/7607

Abstract
We report various many-body theoretical approaches to the nonlinear decay rate and energy loss of charged particles moving in an interacting free electron gas. These include perturbative formulations of the scattering matrix, the self-energy and the induced electron density. Explicit expressions for these quantities are obtained, with inclusion of exchange and correlation effects.

PACS numbers: 45.50.Jf, 71.10.Ca, 05.30.Fk

1. Introduction

The energy loss of non-relativistic charged particles entering a metal is primarily due to the creation of electron–hole pairs and collective excitations in the solid, interactions with the nuclei only becoming important when the velocity of the projectile is much smaller than the mean speed of the electrons in the solid [1].

The degenerate interacting free electron gas (FEG) provides a good model to describe a regime in which electrons are responsible for the energy-loss process. The inelastic decay rate and energy loss of charged particles in FEG have been calculated for many years in the first-Born approximation or, equivalently, within linear response theory. It is well known that these first-order calculations predict an energy loss that grows with the square of the projectile charge, $Z_1 e$, and provide a good approximation when the velocity of the projectile is much larger than the average velocity of the target electrons. However, when the velocity of the projectile decreases non-linearities become apparent. An important example is provided by the existing differences between the energy loss of protons and antiprotons [2–4], which cannot be accounted for within linear-response theory. These differences were then successfully accounted on the basis of second-order perturbative calculations that used the random-phase approximation (RPA) and treated the moving charged particle as a prescribed source of energy

and momentum [5–9]. Beyond-RPA calculations of this so-called Z_1^3 effect have been reported only very recently in the limit of low velocities [10].

In this paper, we report various many-body theoretical approaches to the quadratic decay rate and energy loss of charged particles moving in an interacting FEG, which include exchange-correlation (xc) effects and treat the moving charged particle as part of the many-body interacting system. First of all, we present a fully quantum treatment of the probe particle, which we assume to be distinguishable from the electrons in the Fermi gas. We assign a propagator to this particle, and then follow procedures of many-body perturbation theory to derive explicit expressions for the scattering matrix. From the knowledge of this matrix, both the decay rate and the energy loss of the moving particle can be evaluated either within the RPA or by including short-range xc effects. We also derive an explicit expression for the self-energy of the probe particle, which enables us to present an alternative derivation of the decay rate.

The rest of this paper is organized as follows: A diagrammatic analysis of the decay rate of a moving charged particle in FEG is presented in section 2. The decay rate and stopping power are calculated up to third order in the projectile charge from the knowledge of the scattering matrix. It is shown that for a heavy projectile the decay rate agrees with the imaginary part of the projectile self-energy, and that the stopping power agrees with the result of quadratic-response theory. Our conclusions are presented in section 3. Atomic units are used throughout, i.e., $e^2 = \hbar = m_e = 1$.

2. Diagrammatic analysis

We consider the interaction of a moving probe particle of charge Z_1 and mass M with FEG of density n. The probe particle is assumed to be distinguishable from the electrons in the Fermi gas, which is described by an isotropic homogeneous assembly of interacting electrons immersed in a uniform background of positive charge and volume V.

In the representation of second quantization, the interaction-picture perturbing Hamiltonian reads

$$H_I'(t) = -Z_1 \int \mathrm{d}^3\boldsymbol{r}\,\mathrm{d}^4X\,\psi^\dagger(x)\,\psi(x)\,v(x,X)\,\tilde{\psi}^\dagger(X)\,\tilde{\psi}(X) + \frac{1}{2}\int \mathrm{d}^3\boldsymbol{r}\,\mathrm{d}^4x'\,\psi^\dagger(x)\,\psi(x)\,v(x,x')\,\psi^\dagger(x')\,\psi(x') + H_I^{\mathrm{BG}} \tag{2.1}$$

where $v(x,x')$ $[x = (\boldsymbol{r},t)]$ is the instantaneous Coulomb interaction and the last term represents the interaction of electrons and probe particle with the positive background. The field operators $\psi(x)$ and $\psi^\dagger(x)$ destroy and create an electron at time t and point $\boldsymbol{r}$, while $\tilde{\psi}(X)$ and $\tilde{\psi}^\dagger(X)$ destroy and create the probe particle at time t and point $\boldsymbol{R}$. Annihilation operators can be written as

$$\psi(x) = \sum_i \mathrm{e}^{\mathrm{i}\omega_i t}\,\phi_i(\boldsymbol{r})\,a_i \tag{2.2}$$

and

$$\tilde{\psi}(X) = \sum_i \mathrm{e}^{\mathrm{i}\omega_i t}\,\tilde{\phi}_i(\boldsymbol{R})A_i \tag{2.3}$$

where the operators a_i and A_i annihilate an electron and the probe particle in the one-particle free states $\phi_i(\boldsymbol{r})$ and $\tilde{\phi}_i(\boldsymbol{R})$ of energy ω_i. As we are dealing with a homogeneous system, these states can be taken to be plane-wave states. We choose states of momentum $\boldsymbol{k}$ and energy $\omega_{\boldsymbol{k}} = \boldsymbol{k}^2/2$ for electrons, and momentum $\boldsymbol{p}$ and energy $\omega_{\boldsymbol{p}} = \boldsymbol{p}^2/(2M)$ for the probe particle.

The scattering matrix can be written as a time-ordered exponential [11],

$$S = T\left\{\exp\left[-\mathrm{i}\int_{-\infty}^{\infty} \mathrm{d}t\, \mathrm{e}^{-\eta|t|}\, H_I'(t)\right]\right\} \tag{2.4}$$

where H_I' is the perturbing Hamiltonian of equation (2.1), T is the chronological operator and η is a positive infinitesimal.

In the interaction picture, electron and probe-particle propagators can be expressed as

$$G(x, x') = -\mathrm{i}\,\frac{\langle 0, \Phi_0|\, T\, \psi_I(x)\, \psi_I^\dagger(x')\, S\, |0, \Phi_0\rangle}{\langle 0, \Phi_0|\, S\, |0, \Phi_0\rangle} \tag{2.5}$$

and

$$D(X, X') = -\mathrm{i}\,\frac{\langle 0, \Phi_0|\, T\, \psi_I(X)\, \psi_I^\dagger(X')\, S\, |0, \Phi_0\rangle}{\langle 0, \Phi_0|\, S\, |0, \Phi_0\rangle} \tag{2.6}$$

where $|0, \Phi_0\rangle = |0\rangle|\Phi_0\rangle$ represents the non-interacting free Fermi sea with no probe particle. Non-interacting electron and probe-particle propagators are easily found from equations (2.5) and (2.6) given by the following simple expressions:

$$G^0(x, x') = -\mathrm{i}\,\langle \Phi_0|\, T\, \psi(x)\, \psi^\dagger(x')\, |\Phi_0\rangle \tag{2.7}$$

and

$$D^0(X, X') = -\mathrm{i}\,\langle 0|\, T\, \psi(X)\, \psi^\dagger(X')\, |0\rangle \tag{2.8}$$

respectively.

We note that the probe-particle propagator is a retarded function, i.e., it is different from zero only if $t > t'$. As a consequence, probe-particle bubbles do not contribute to the diagrammatic expansion. Therefore, the expansion of equation (2.6) does not depend on whether the probe particle is a fermion or a boson, and there is no probe-particle contribution to the denominator of equations (2.5) and (2.6).

2.1. Scattering approach

Let us consider the process corresponding to the creation of a single electron–hole pair where the system is carried from an initial state $A_i^\dagger\, |0, \Phi_0\rangle$ to a final state $a_{f_1}^\dagger a_{i_1} A_f^\dagger\, |0, \Phi_0\rangle$. The scattering-matrix element for this process is

$$S_{f, f_1; i, i_1} = \frac{\langle 0, \Phi_0|\, a_{f_1}\, a_{i_1}^\dagger\, A_f\, S\, A_i^\dagger\, |0, \Phi_0\rangle}{\langle 0, \Phi_0|\, S\, |0, \Phi_0\rangle}. \tag{2.9}$$

Similarly, one may consider a double excitation in which the system is carried from an initial state $A_i^\dagger\, |0, \Phi_0\rangle$ to a final state $a_{f_1}^\dagger a_{f_2}^\dagger a_{i_1} a_{i_2} A_f^\dagger\, |0, \Phi_0\rangle$. The matrix element for this process is

$$S_{f, f_1, f_2; i, i_1, i_2} = \frac{\langle 0, \Phi_0|\, a_{f_1}\, a_{f_2}\, a_{i_1}^\dagger\, a_{i_2}^\dagger\, A_f\, S\, A_i^\dagger\, |0, \Phi_0\rangle}{\langle 0, \Phi_0|\, S\, |0, \Phi_0\rangle}. \tag{2.10}$$

After introduction of the Hamiltonian of equation (2.1) into equation (2.4), the matrix elements $S_{f, f_1; i, i_1}$ and $S_{f, f_1, f_2; i, i_1, i_2}$ of equations (2.9) and (2.10) can be expanded in powers of the coupling constant e^2. Then, the use of Wick's theorem yields explicit expressions for the various contributions to this expansion, in terms of the non-interacting propagators $G^0(x, x')$ and $D^0(X, X')$. Introducing standard Fourier representations and taking the free-particle states to be momentum eigenfunctions, all contributions to the scattering matrix can be derived from scattering-like Feynman diagrams as follows:

1. Draw all distinct scattering diagrams in momentum space. All particle lines must be directed. Different ways of directing them that are not topologically equivalent give distinct contributions. Exclude probe-particle bubbles.
2. Assign momentum and energy to all particle and interaction lines so that the sum of the four-momenta entering a vertex equals the sum of four-momenta leaving the vertex.
3. Include an overall factor $2\pi\, V\, \delta_{\boldsymbol{k}}\, \delta(k^0)$, which represents total momentum and energy conservation. $\delta_{\boldsymbol{k}}$ is the Kronecker δ symbol and $\delta(k^0)$ is the Dirac δ function.
4. For every external particle line include a factor $V^{-1/2}$.
5. For every internal electron line include $i\,G_k^0$, where G_k^0 is the non-interacting one-electron propagator in momentum space:

$$G_k^0 = \frac{1-n_{\boldsymbol{k}}}{k^0-\omega_{\boldsymbol{k}}+\mathrm{i}\eta} + \frac{n_{\boldsymbol{k}}}{k^0-\omega_{\boldsymbol{k}}-\mathrm{i}\eta} \tag{2.11}$$

   $(\boldsymbol{k}, k^0)$ being the four-momentum of the particle, $n_{\boldsymbol{k}}$ the occupation number ($n_{\boldsymbol{k}} = \Theta(q_{\mathrm{F}} - |\boldsymbol{q}|)$, where q_{F} is the Fermi momentum) and $\omega_{\boldsymbol{k}} = \boldsymbol{k}^2/2$.
6. For every internal probe-particle line include a factor $\mathrm{i}D_p^0$, where D_p^0 is the non-interacting probe-particle propagator in momentum space:

$$D_p^0 = \frac{1}{p^0-\omega_{\boldsymbol{p}}+\mathrm{i}\eta} \tag{2.12}$$

   $(\boldsymbol{p},\, p^0)$ being the four-momentum of the particle, and $\omega_{\boldsymbol{p}} = \boldsymbol{p}^2/(2M)$.
7. For every probe_particle–electron and electron–electron interaction line, include a factor $\mathrm{i}Z_1 v_{\boldsymbol{q}}$ and $-\mathrm{i}v_{\boldsymbol{q}}$ respectively, $v_{\boldsymbol{q}}$ being the Fourier transform of the bare Coulomb potential.
8. For every electron loop include a factor -2.
9. Integrate over free four-momenta, $\int \mathrm{d}^4q/(2\pi)^4$.

Since all scattering-matrix elements include delta functions accounting for momentum and energy conservation, one may factorize them as follows:

$$S_{f,f_1;i,i_1} = 2\pi\delta_{\boldsymbol{p}_f-\boldsymbol{p}_i-\boldsymbol{k}_{f_1}+\boldsymbol{k}_{i_1}}\,\delta\left(\omega_{\boldsymbol{p}_f}-\omega_{\boldsymbol{p}_i}-\omega_{\boldsymbol{k}_{f_1}}+\omega_{\boldsymbol{k}_{i_1}}\right)T_{f,f_1;i,i_1} \tag{2.13}$$

and

$$\begin{aligned} S_{f,f_1,f_2;i,i_1,i_2} &= 2\pi\delta_{\boldsymbol{p}_f-\boldsymbol{p}_i-\boldsymbol{k}_{f_1}-\boldsymbol{k}_{f_2}+\boldsymbol{k}_{i_1}+\boldsymbol{k}_{i_2}}\,\delta\left(\omega_{\boldsymbol{p}_f}-\omega_{\boldsymbol{p}_i}-\omega_{\boldsymbol{k}_{f_1}}-\omega_{\boldsymbol{k}_{f_2}}+\omega_{\boldsymbol{k}_{i_1}}+\omega_{\boldsymbol{k}_{i_2}}\right) \\ &\quad\times T_{f,f_1,f_2;i,i_1,i_2} \end{aligned} \tag{2.14}$$

where $\boldsymbol{k}_{i_1,i_2,f_1,f_2}$ and $\boldsymbol{p}_{i,f}$ represent the initial and final momenta of target electrons and probe particle, respectively, with energies $\omega_{\boldsymbol{k}_{i_1,i_2,f_1,f_2}} = \boldsymbol{k}^2_{i_1,i_2,f_1,f_2}/2$ and $\omega_{\boldsymbol{p}_{i,f}} = \boldsymbol{p}^2_{i,f}/(2M)$.

The probabilities $\gamma_q^{\mathrm{single}}$ and $\gamma_q^{\mathrm{double}}$ for the probe particle to transfer four-momentum q ($q^0 > 0$) to FEG by creating single and double excitations are derived by summing the matrix elements over all available initial and final electron states and all final probe-particle states [8]:

$$\gamma_q^{\mathrm{single}} = 4\pi\sum_{\boldsymbol{k}} n_{\boldsymbol{k}}\,(1-n_{\boldsymbol{k}+\boldsymbol{q}})\,|T_{\boldsymbol{q},\boldsymbol{k}}(p_i)|^2\delta\left(q^0+\omega_{\boldsymbol{k}}-\omega_{\boldsymbol{k}+\boldsymbol{q}}\right)\delta[q^0-\boldsymbol{q}\cdot\boldsymbol{v}+q^2/(2M)] \tag{2.15}$$

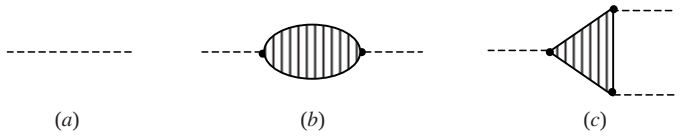

Figure 1. (*a*) Direct, (*b*) linear and (*c*) quadratic contributions to the screened interaction. Dashed lines represent the bare Coulomb interaction, $-i v_{\boldsymbol{q}}$. Two- and three-point loops represent time-ordered density correlation functions $i\chi_q$ and $-2\,Y_{q_1,q_2}$, respectively.

and

$$\gamma_q^{\text{double}} = 8\pi \sum_{\boldsymbol{q}_1} \int \mathrm{d}q_1^0 \sum_{\boldsymbol{k}_1} \sum_{\boldsymbol{k}_2} n_{\boldsymbol{k}_1} \left(1 - n_{\boldsymbol{k}_1+\boldsymbol{q}_1}\right) n_{\boldsymbol{k}_2} \left(1 - n_{\boldsymbol{k}_2+\boldsymbol{q}-\boldsymbol{q}_1}\right) |T_{\boldsymbol{q},\boldsymbol{q}_1,\boldsymbol{k}_1,\boldsymbol{k}_2}(p_i)|^2 \times \delta\left(q_1^0 + \omega_{\boldsymbol{k}_1} - \omega_{\boldsymbol{k}_1+\boldsymbol{q}_1}\right) \delta\left(q^0 - q_1^0 + \omega_{\boldsymbol{k}_2} - \omega_{\boldsymbol{k}_2+\boldsymbol{q}-\boldsymbol{q}_1}\right) \times \delta[q^0 - \boldsymbol{q}\cdot\boldsymbol{v} + q^2/(2M)] \tag{2.16}$$

where $\boldsymbol{v}$ represents the velocity of the probe particle.

In these equations recoil has not been neglected. Moreover, the quantum character of the probe particle is implicit in the T-matrix elements, which include the probe-particle propagator $D^0(p)$. Therefore, they generalize the results of reference [8] to the case of an arbitrary distinguishable probe particle.

Hence, the total decay rate of the probe charge is given by the following expression:

$$\tau^{-1}(p) = \sum_{\boldsymbol{q}} \int_0^\infty \mathrm{d}q^0 \left[\gamma_q^{\text{single}} + \gamma_q^{\text{double}} + \cdots\right]. \tag{2.17}$$

The average energy lost per unit length travelled by the probe particle, i.e., the so-called stopping power of the target is obtained by inserting q^0/v inside the integrand in equation (2.17):

$$-\frac{\mathrm{d}E}{\mathrm{d}x}(p) = \frac{1}{v} \sum_{\boldsymbol{q}} \int_0^\infty \mathrm{d}q^0\, q^0 \left[\gamma_q^{\text{single}} + \gamma_q^{\text{double}} + \cdots\right]. \tag{2.18}$$

It is well known that the decay rate and energy loss cannot be computed by simply evaluating the lowest-order tree-level Feynman diagrams because of severe infrared divergences due to the long-range Coulomb interaction. Instead, one needs to resume electron-loop corrections and expand the scattering matrix in terms of the dynamically screened Coulomb interaction.

Direct, linear and quadratic contributions to the screened interaction are represented in figure 1. Dashed lines $[-i v_{\boldsymbol{q}}]$ represent the bare Coulomb interaction. The full bubble and triangle, denoted $\mathrm{i}\chi_q$ and $-2\,Y_{q_1,q_2}$, represent the sum of all possible Feynman diagrams joining two and three points, and thus correspond to the Fourier transform of time-ordered density correlation functions of the interacting FEG:

$$\chi_q = \int \mathrm{d}^4x_1\, \mathrm{e}^{-\mathrm{i}[\boldsymbol{q}\cdot(\boldsymbol{r}_1-\boldsymbol{r}_2)-q^0(t_1-t_2)]}\, \chi(x_1, x_2) \tag{2.19}$$

and

$$Y_{q_1,q_2} = \int \mathrm{d}^4x_1 \int \mathrm{d}^4x_2\, \mathrm{e}^{-\mathrm{i}[\boldsymbol{q}_1\cdot(\boldsymbol{r}_1-\boldsymbol{r}_2)-q_1^0(t_1-t_2)]}\, \mathrm{e}^{-\mathrm{i}\left[(\boldsymbol{q}_1+\boldsymbol{q}_2)\cdot(\boldsymbol{r}_2-\boldsymbol{r}_3)-\left(q_1^0+q_2^0\right)(t_2-t_3)\right]} Y(x_1, x_2, x_3) \tag{2.20}$$

with

$$\chi(x, x') = -\mathrm{i}\langle\Psi_0|T\,\tilde{\rho}_{\mathrm{H}}(x)\tilde{\rho}_{\mathrm{H}}(x')|\Psi_0\rangle \tag{2.21}$$

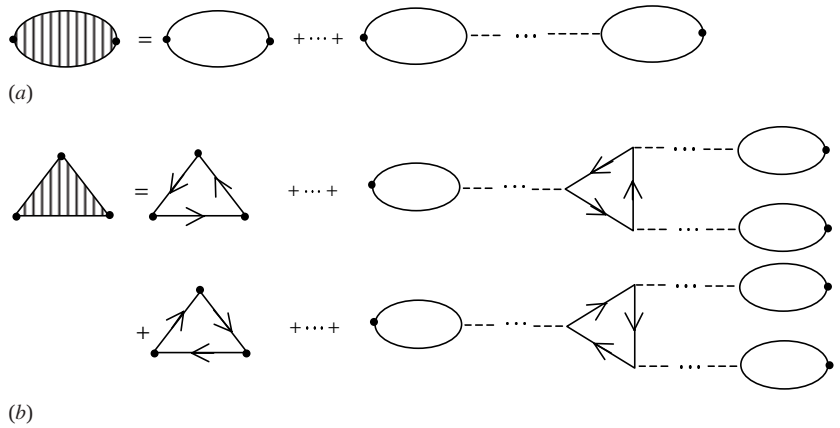

Figure 2. (*a*) The interacting RPA two-point density correlation function, represented by a full bubble, is obtained by summing over the infinite set of diagrams that contain a string of empty bubbles. (*b*) The interacting RPA three-point density correlation function, represented by a full triangle, is obtained by summing over the infinite set of diagrams that combine three strings of empty bubbles through an empty triangle.

and

$$Y(x,x',x'') = -\tfrac{1}{2}\langle\Psi_0|T\,\tilde{\rho}_{\rm H}(x)\tilde{\rho}_{\rm H}(x')\tilde{\rho}_{\rm H}(x'')|\Psi_0\rangle. \tag{2.22}$$

Here, $|\Psi_0\rangle$ represents the normalized exact many-electron ground state, and $\tilde{\rho}_{\rm H}(x) = \hat{\rho}_{\rm H}(x) - n$ is the exact Heisenberg electron-density fluctuation operator, both in the absence of probe particle.

Introducing complete sets of energy eigenstates between the Heisenberg fields of equations (2.21) and (2.22), one obtains spectral representations for χ_q and Y_{q_1,q_2}. We find

$$\chi_q = V^{-1}\sum_n \left|(\rho_{\boldsymbol{q}})_{n0}\right|^2\left[\frac{1}{q^0-\omega_{n0}+{\rm i}\eta_{q^0}} - \frac{1}{q^0+\omega_{n0}+{\rm i}\eta_{q^0}}\right] \tag{2.23}$$

and

$$\begin{aligned} Y_{q_1,q_2} = -\frac{1}{2}\,V^{-1}\sum_{n,l}\Bigg[& \frac{(\rho_{\boldsymbol{q}_1})_{0n}\,(\rho_{\boldsymbol{q}_3})_{nl}\,(\rho_{\boldsymbol{q}_2})_{l0}}{\left(q_1^0-\omega_{n0}+{\rm i}\eta_{q_1^0}\right)\left(q_2^0+\omega_{l0}+{\rm i}\eta_{q_2^0}\right)} \\ & + \frac{(\rho_{\boldsymbol{q}_2})_{0n}\,(\rho_{\boldsymbol{q}_1})_{nl}\,(\rho_{\boldsymbol{q}_3})_{l0}}{\left(q_2^0-\omega_{n0}+{\rm i}\eta_{q_2^0}\right)\left(q_3^0+\omega_{l0}+{\rm i}\eta_{q_3^0}\right)} \\ & + \frac{(\rho_{\boldsymbol{q}_3})_{0n}\,(\rho_{\boldsymbol{q}_2})_{nl}\,(\rho_{\boldsymbol{q}_1})_{l0}}{\left(q_3^0-\omega_{n0}+{\rm i}\eta_{q_3^0}\right)\left(q_1^0+\omega_{l0}+{\rm i}\eta_{q_1^0}\right)} + (q_2\to q_3)\Bigg] \end{aligned} \tag{2.24}$$

where $\eta_q = \eta\ \mathrm{sgn}(q^0)$, $\omega_{nl} = E_n - E_l$, $q_3 = -(q_1+q_2)$ and $(\rho_{\boldsymbol{q}})_{nl}$ is the matrix element of the Fourier transform of the electron-density operator taken between exact many-electron states of energy E_n and E_l.

In the RPA, density correlation functions are obtained by summing over all ring-like diagrams, as shown in figure 2, thereby neglecting all self-energy, vertex and vertex-ladder insertions (see figure 3). Hence,

$$\chi_q^{\rm RPA} = \chi_q^0 + \chi_q^0\,v_{\boldsymbol{q}}\,\chi_q^{\rm RPA} \tag{2.25}$$

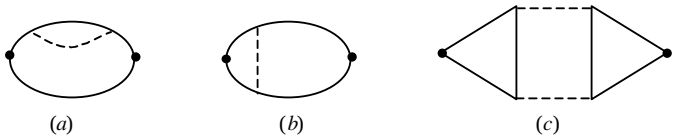

Figure 3. (*a*) Self-energy, (*b*) vertex and (*c*) ladder insertions, which are neglected within RPA.

and

$$Y^{\mathrm{RPA}}_{q_1,q_2} = K^{\mathrm{RPA}}_{q_1}\, Y^{0}_{q_1,q_2}\, K^{\mathrm{RPA}}_{-q_2}\, K^{\mathrm{RPA}}_{-q_3} \tag{2.26}$$

where χ^0_q and $Y^0_{q_1,q_2}$ are the non-interacting FEG density correlation functions and K_q is the so-called inverse dielectric function:

$$K^{\mathrm{RPA}}_q = 1 + \chi^{\mathrm{RPA}}_q\, v_{\boldsymbol{q}}. \tag{2.27}$$

Improvements on the RPA are typically carried out by introducing an effective e–e interaction [12],

$$\tilde{v}_q = v_{\boldsymbol{q}}\left(1 - G_q\right) \tag{2.28}$$

where G_q is the so-called local-field factor, first introduced by Hubbard [13], accounting for all self-energy, vertex and vertex-ladder insertions not present in the RPA. Accordingly, the density correlation functions χ_q and Y_{q_1,q_2} are found to be of the RPA form, but with all e–e bare Coulomb interactions $v_{\boldsymbol{q}}$ replaced by $\tilde{v}_q$ [14]:

$$\chi_q = \chi^0_q + \chi^0_q\, \tilde{v}_q\, \chi_q \tag{2.29}$$

and

$$Y_{q_1,q_2} = \tilde{K}_{q_1}\, Y^0_{q_1,q_2}\, \tilde{K}_{-q_2}\, \tilde{K}_{-q_3} \tag{2.30}$$

where the so-called test_charge–electron inverse dielectric function has been introduced [15, 16]:

$$\tilde{K}_q = 1 + \chi_q\, \tilde{v}_q. \tag{2.31}$$

This inverse dielectric function screens the potential generated by a distinguishable test charge and 'felt' by an electron, whereas the so-called test_charge–test_charge inverse dielectric function K_q of equation (2.27) screens the potential both generated and 'felt' by a distinguishable test charge:

$$K_q = 1 + \chi_q\, v_q. \tag{2.32}$$

Now we proceed to expand the matrix elements of equations (2.9) and (2.10) in powers of the dynamically screened Coulomb interaction. At this point, we will only introduce self-energy and vertex insertions that can be described with the use of a static local-field factor [$G_q \to G_{\boldsymbol{q},0}$]. Within this approximation, all processes corresponding to the creation of single and double excitations can be represented by diagrams of figure 4 (as in the RPA there are no contributions, up to second order in Z_1, from third- and higher-order excitations [8]). Thus, one finds

$$\begin{aligned} T_{\boldsymbol{q},\boldsymbol{k}} = {} & \mathrm{i}\, Z_1\, V^{-1}\, v_{\boldsymbol{q}}\, \tilde{K}_q + Z_1^2\, V^{-1} \int \frac{\mathrm{d}^4 q_1}{(2\pi)^4} \Big[2\, \tilde{v}_q\, v_{\boldsymbol{q}_1}\, v_{\boldsymbol{q}-\boldsymbol{q}_1}\, D^0_{p-q_1}\, Y_{q,-q_1} \\ & + v_{\boldsymbol{q}_1}\, \tilde{K}_{q_1}\, v_{\boldsymbol{q}-\boldsymbol{q}_1}\, \tilde{K}_{q-q_1}\, D^0_{p-q_1} \left(G^0_{k+q_1} + G^0_{k+q-q_1} \right) \Big] \end{aligned} \tag{2.33}$$

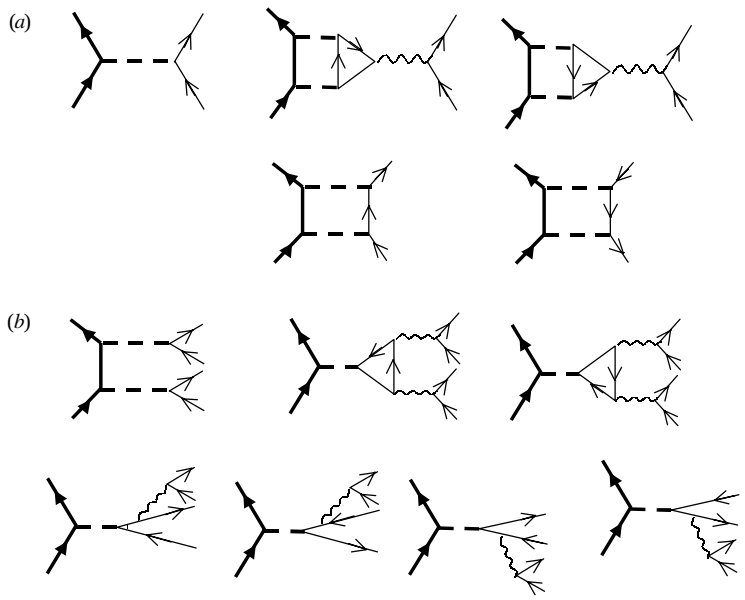

Figure 4. Diagrammatic representation of the scattering-matrix elements of (*a*) equation (2.33) and (*b*) equation (2.34). Thick and thin solid lines represent non-interacting probe-particle and electron propagators, iD^0_p and iG^0_k, respectively. Wiggly lines represent the screened e–e Coulomb interaction, $-i\tilde{v}_{\boldsymbol{q}}\tilde{K}_q$, and thick discontinuous lines represent the screened interaction between electrons and probe particle, $-iv_{\boldsymbol{q}}\tilde{K}_q$

and

$$T_{\boldsymbol{q},\boldsymbol{q}_1,\boldsymbol{k}_1,\boldsymbol{k}_2} = i\,Z_1\,V^{-2}\left[2\,v_{\boldsymbol{q}}\,\tilde{v}_{q_1}\,\tilde{v}_{q-q_1}\,Y_{q,-q_1} + v_{\boldsymbol{q}}\,\tilde{K}_q\,v_{\boldsymbol{q}-\boldsymbol{q}_1}\,\tilde{K}_{q-q_1}\left(G^0_{k_1+q} + G^0_{k_1-q+q_1}\right)\right.$$
$$\left. + v_{\boldsymbol{q}}\,\tilde{K}_q\,v_{\boldsymbol{q}_1}\,\tilde{K}_{q_1}\left(G^0_{k_2+q} + G^0_{k_2-q_1}\right)\right]$$
$$- i\,Z_1^2\,V^{-2}\,v_{\boldsymbol{q}_1}\,\tilde{K}_{q_1}\,v_{\boldsymbol{q}-\boldsymbol{q}_1}\,\tilde{K}_{q-q_1}\,D^0_{p-q_1}. \tag{2.34}$$

As static local-field factors are known to be real ($\mathrm{Im}\,G_{\boldsymbol{q},0} = 0$), one easily finds

$$\mathrm{Im}\,K_q = v_{\boldsymbol{q}}\,|\tilde{K}_q|^2\,\mathrm{Im}\,\chi^0_q \tag{2.35}$$

and

$$\mathrm{Im}\,\tilde{K}_q = \tilde{v}_q\,|\tilde{K}_q|^2\,\mathrm{Im}\,\chi^0_q \tag{2.36}$$

where K_q and $\tilde{K}_q$ are the inverse dielectric functions of equations (2.27) and (2.32), with the density correlation function χ_q being given in both cases by equation (2.29).

Introduction of equations (2.33) and (2.34) into equations (2.15) and (2.16) yields the following results, valid up to third order in the probe_particle–electron screened interaction:

$$\gamma_q^{\mathrm{single}} = -2\,Z_1^2\,V^{-1}\,v_{\boldsymbol{q}}\left\{\mathrm{Im}\,K_q + 4\,Z_1\int\frac{\mathrm{d}^4q_1}{(2\pi)^4}\,v_{\boldsymbol{q}_1}\,v_{\boldsymbol{q}-\boldsymbol{q}_1}\Big[\mathrm{Im}\,\tilde{K}_q\right.$$
$$\left.\times\,\mathrm{Im}\left(D^0_{p-q_1}\,Y^0_{q,-q_1}\,\tilde{K}_{q_1}\,\tilde{K}_{q-q_1}\right) + \mathrm{Im}\left(\tilde{K}^*_q\,\tilde{K}_{q_1}\,\tilde{K}_{q-q_1}\,D^0_{p-q_1}\,I_{q,q_1}\right)\Big]\right\}$$
$$\times\,\delta[q^0 - \boldsymbol{q}\cdot\boldsymbol{v} + q^2/(2M)]\,\Theta(q^0) \tag{2.37}$$

and

$$\gamma_q^{\text{double}} = -16\, Z_1^3\, V^{-1}\, v_{\boldsymbol{q}} \int \frac{\mathrm{d}^4 q_1}{(2\pi)^4}\, v_{\boldsymbol{q}_1}\, v_{\boldsymbol{q}-\boldsymbol{q}_1} \left\{ \operatorname{Im} \tilde{K}_{q_1} \operatorname{Im} \tilde{K}_{q-q_1} \operatorname{Re}\left(\tilde{K}_q\, D^{0*}_{p-q_1}\, Y^0_{q,-q_1} \right) \right.$$
$$\left. + \operatorname{Im} \tilde{K}_{q-q_1} \operatorname{Re}\left[\tilde{K}_q\, \tilde{K}^*_{q_1} \left(D^{0*}_{p-q_1} + D^{0*}_{p-q+q_1} \right) I_{q_1,q} \right] \right\}$$
$$\times\, \delta[q^0 - \boldsymbol{q}\cdot\boldsymbol{v} + q^2/(2M)]\, \Theta\left(q_1^0\right)\, \Theta\left(q^0 - q_1^0\right) \tag{2.38}$$

where we have defined the function I_{q,q_1} as

$$I_{q,q_1} = \tfrac{1}{2}\left[H_{q,q_1} + H_{q,q-q_1} + \mathrm{i}\left(J_{q,q_1} + J_{q,q-q_1} \right) \right] \tag{2.39}$$

with

$$H_{q,q_1} = -2\pi\, V^{-1} \sum_{\boldsymbol{k}} n_{\boldsymbol{k}}\, (1 - n_{\boldsymbol{k}+q}) \left[\frac{\delta\left(q^0 + \omega_{\boldsymbol{k}} - \omega_{\boldsymbol{k}+\boldsymbol{q}}\right)}{q_1^0 + \omega_{\boldsymbol{k}} - \omega_{\boldsymbol{k}+\boldsymbol{q}_1}} - \frac{\delta\left(q^0 - \omega_{\boldsymbol{k}} + \omega_{\boldsymbol{k}+\boldsymbol{q}}\right)}{q_1^0 - \omega_{\boldsymbol{k}} + \omega_{\boldsymbol{k}+\boldsymbol{q}_1}} \right] \tag{2.40}$$

and

$$J_{q,q_1} = 2\pi^2\, V^{-1} \sum_{\boldsymbol{k}} n_{\boldsymbol{k}}\, (1 - n_{\boldsymbol{k}+\boldsymbol{q}}) \delta\left(q^0 + \omega_{\boldsymbol{k}} - \omega_{\boldsymbol{k}+\boldsymbol{q}}\right) \left[(1 - n_{\boldsymbol{k}+\boldsymbol{q}_1})\, \delta\left(q_1^0 + \omega_{\boldsymbol{k}} - \omega_{\boldsymbol{k}+\boldsymbol{q}_1}\right) \right.$$
$$\left. - n_{\boldsymbol{k}+\boldsymbol{q}-\boldsymbol{q}_1}\, \delta\left(q^0 - q_1^0 + \omega_{\boldsymbol{k}} - \omega_{\boldsymbol{k}+\boldsymbol{q}-\boldsymbol{q}_1}\right) \right]. \tag{2.41}$$

Introduction of equations (2.37) and (2.38) into equations (2.17) and (2.18) yields the total decay rate and the average energy loss of arbitrary particles that are distinguishable from the electrons in the Fermi gas, with inclusion of static many-body local-field effects.

In order to compare our result with previous work, we now consider the case where the probe particle is very heavy ($M \gg 1$) and recoil can be neglected, i.e., $\omega_{\boldsymbol{p}} - \omega_{\boldsymbol{p}-\boldsymbol{q}} \sim \boldsymbol{q}\cdot\boldsymbol{v}$. In this approximation, the principal part of the non-interacting probe-particle propagator is found to give no contribution to the integrals of equations (2.37) and (2.38), and one finds

$$\gamma_q^{\text{single}} = 2\, Z_1^2\, V^{-1}\, v_{\boldsymbol{q}} \left\{ -\operatorname{Im} K_q + 4\pi\, Z_1 \int \frac{\mathrm{d}^4 q_1}{(2\pi)^4}\, v_{\boldsymbol{q}_1}\, v_{\boldsymbol{q}-\boldsymbol{q}_1}\, \delta\left(q_1^0 - \boldsymbol{q}_1\cdot\boldsymbol{v}\right) \right.$$
$$\left. \times \left[\operatorname{Im} \tilde{K}_q \operatorname{Re}\left(Y^0_{q,-q_1}\, \tilde{K}_{q_1}\, \tilde{K}_{q-q_1} \right) + \operatorname{Re}(\tilde{K}_q{}^*\, \tilde{K}_{q_1} \tilde{K}_{q-q_1}\, I_{q,q_1}) \right] \right\}$$
$$\times\, \delta(q^0 - \boldsymbol{q}\cdot\boldsymbol{v})\, \Theta(q^0) \tag{2.42}$$

and

$$\gamma_q^{\text{double}} = 16\pi\, Z_1^3\, V^{-1}\, v_{\boldsymbol{q}} \int \frac{\mathrm{d}^4 q_1}{(2\pi)^4}\, v_{\boldsymbol{q}_1}\, v_{\boldsymbol{q}-\boldsymbol{q}_1} \left[\operatorname{Im} \tilde{K}_{q_1} \operatorname{Im} \tilde{K}_{q-q_1} \operatorname{Im}\left(\tilde{K}_q\, Y^0_{q,-q_1} \right) \right.$$
$$\left. + 2 \operatorname{Im} \tilde{K}_{q-q_1} \operatorname{Im}(\tilde{K}_q\, \tilde{K}^*_{q_1}\, I_{q_1,q}) \right]$$
$$\times\, \delta\left(q_1^0 - \boldsymbol{q}_1\cdot\boldsymbol{v}\right)\, \delta(q^0 - \boldsymbol{q}\cdot\boldsymbol{v})\, \Theta\left(q_1^0\right)\, \Theta\left(q^0 - q_1^0\right). \tag{2.43}$$

These decay probabilities, which account for the existence of many-body static local-field corrections, coincide in the RPA ($G_q = 0$) with those derived in reference [9] by treating the probe particle as a prescribed source of energy and momentum.

Simplified expressions for the total decay rate and the average energy loss of heavy ($M \gg 1$) probe particles can be obtained with the aid of the following relationship, obtained in reference [9], which relates the imaginary part of the non-interacting density correlation function $Y^0_{q_1,q_2}$ with the function H_{q,q_1} of equation (2.40)

$$\operatorname{Im} Y^0_{q_1,q_2} = \tfrac{1}{2}\left[H_{q_1,-q_2} + H_{-q_2,q_1} + H_{-q_3,q_2} + (q_2 \to q_3) \right]. \tag{2.44}$$

Introduction of equations (2.42) and (2.43) into equations (2.17) and (2.18) yields, after some algebra,

$$\tau^{-1} = 4\pi\, Z_1^2 \int \frac{\mathrm{d}^4 q}{(2\pi)^4}\, v_{\boldsymbol{q}} \left\{ -\mathrm{Im}\, K_q + 4\pi\, Z_1 \int \frac{\mathrm{d}^4 q_1}{(2\pi)^4}\, v_{\boldsymbol{q}_1}\, v_{\boldsymbol{q}-\boldsymbol{q}_1}\, \delta\left(q_1^0 - \boldsymbol{q}_1 \cdot \boldsymbol{v}\right) \right.$$
$$\left. \times \left[f_1(q,q_1) + f_2(q,q_1) + f_3^a(q,q_1) + f_3^b(q,q_1) + f_4(q,q_1) \right] \right\}$$
$$\times\, \delta(q^0 - \boldsymbol{q}\cdot\boldsymbol{v})\, \Theta(q^0) \tag{2.45}$$

and[1]

$$-\frac{\mathrm{d}E}{\mathrm{d}x} = \frac{4\pi}{v}\, Z_1^2 \int \frac{\mathrm{d}^4 q}{(2\pi)^4}\, q^0\, v_{\boldsymbol{q}} \left\{ -\mathrm{Im}\, K_q + 4\pi\, Z_1 \int \frac{\mathrm{d}^4 q_1}{(2\pi)^4}\, v_{\boldsymbol{q}_1}\, v_{\boldsymbol{q}-\boldsymbol{q}_1}\, \delta\left(q_1^0 - \boldsymbol{q}_1 \cdot \boldsymbol{v}\right) \right.$$
$$\left. \times \left[f_1(q,q_1) + f_2(q,q_1) + f_3^a(q,q_1) + f_5(q,q_1) \right] \right\}$$
$$\times\, \delta(q^0 - \boldsymbol{q}\cdot\boldsymbol{v})\, \Theta(q^0) \tag{2.46}$$

where

$$f_1(q,q_1) = \mathrm{Im}\, \tilde{K}_q\ \mathrm{Re}\, Y^0_{q,-q_1}\ \mathrm{Re}\, \tilde{K}_{q_1}\ \mathrm{Re}\, \tilde{K}_{q-q_1} \tag{2.47}$$
$$f_2(q,q_1) = \mathrm{Re}\, \tilde{K}_q\ H_{q,q_1}\ \mathrm{Re}\, \tilde{K}_{q_1}\ \mathrm{Re}\, \tilde{K}_{q-q_1} \tag{2.48}$$
$$f_3^a(q,q_1) = -2\ \mathrm{Im}\, \tilde{K}_q\ H_{q_1,q}\ \mathrm{Im}\, \tilde{K}_{q_1}\ \mathrm{Re}\, \tilde{K}_{q-q_1} \tag{2.49}$$
$$f_3^b(q,q_1) = -\mathrm{Re}\, \tilde{K}_q\ H_{q,q_1}\ \mathrm{Im}\, \tilde{K}_{q_1}\ \mathrm{Im}\, \tilde{K}_{q-q_1} \tag{2.50}$$
$$f_4(q,q_1) = -\tfrac{1}{3}\ \mathrm{Im}\, \tilde{K}_q\ \mathrm{Re}\, Y^0_{q,-q_1}\ \mathrm{Im}\, \tilde{K}_{q_1}\ \mathrm{Im}\, \tilde{K}_{q-q_1} \tag{2.51}$$

and

$$f_5(q,q_1) = \mathrm{Im}\left(\tilde{K}_q \tilde{K}^*_{q_1} \tilde{K}_{q-q_1} \right) J_{q-q_1,-q_1}. \tag{2.52}$$

Within RPA, the inverse dielectric functions K_q and $\tilde{K}_q$ coincide and equation (2.46) reduces to the result of reference [8].

Equation (2.45) has not been reported before, even within the RPA approximation. In next section we will show that it is equivalent to the result reported in reference [10], where a derivation of the decay rate as the imaginary part of the on-shell self-energy of the probe particle was sketched briefly.

2.2. Self-energy approach

Since we are considering the interaction of a moving probe particle with a spatially uniform electron gas, invariant under translations, the exact probe-particle propagator can be written in the form of an algebraic Dyson's equation [11]

$$D_p = D_p^0 + D_p^0\, \Sigma_p\, D_p \tag{2.53}$$

which defines the self-energy Σ_p of the probe particle. With the aid of equation (2.12), Dyson's equation can be solved explicitly as

$$D_p = \frac{1}{p^0 - \omega_{\boldsymbol{p}} - \Sigma_p + \mathrm{i}\eta}. \tag{2.54}$$

[1] The term $f_5(q,q_1)$ of equation (2.46) is missing in equation (4.13) of reference [9]. This contribution to the energy loss is found to be negligible at low and high velocities, and the inclusion of this term results, within RPA, in a Z_1^3 correction to the stopping power that is at intermediate velocities lower than that reported in reference [9] by less than 10%. We note that the symmetrized empty three-point function defined in reference [9] is $M_{q,q_1} = -Y^0_{q,-q_1}$.

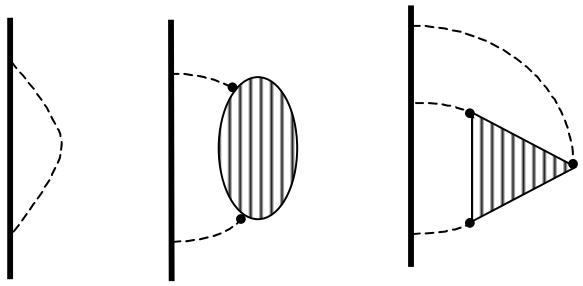

Figure 5. The probe particle self-energy, up to third order in Z_1. Thick solid lines represent the exact probe-particle propagator, $\mathrm{i}D_p$. Dashed lines represent the bare Coulomb interaction, $-\mathrm{i}\,v_{\boldsymbol{q}}$. Two- and three-point loops represent time-ordered density correlation functions, $\mathrm{i}\,\chi_q$ and $-2\,Y_{q_1,q_2}$, respectively.

The energy and lifetime of the excited state (quasi-particle) obtained by adding a particle to an interacting ground state are determined by the poles of the analytical continuation of the one-particle Green function. Hence, the energy of the quasi-particle is $\omega_{\boldsymbol{p}} + \mathrm{Re}\Sigma_{\mathrm{p}}$, and the probability for it to occupy a given excited state decays exponentially in time with the decay constant

$$\tau^{-1} = -2\,\mathrm{Im}\Sigma_p \tag{2.55}$$

with the self-energy calculated at the pole of the one-particle propagator D_p.

The self-energy can be represented diagrammatically as the sum of the so-called proper self-energy insertions, i.e., all Feynman diagrams that cannot be separated into two pieces by cutting a single particle line. Since the probe particle, of charge Z_1, is assumed to be distinguishable from the electrons in the Fermi sea, the self-energy may be expanded in powers of Z_1, diagrams of order Z_1^n containing $n-1$ probe-particle propagators. For a homogeneous electron gas, contributions from the uniform positive background are cancelled by the sum of the so-called 'tadpole' diagrams; therefore, after resuming all electron-loop corrections, the self-energy of the probe particle can be represented diagrammatically up to third order in Z_1 as in figure 5. The sum of the first two diagrams represents the so-called GW approximation, and the third diagram accounts for Z_1^3 corrections to the decay rate of the quasi-particle. One finds

$$\Sigma_p = \mathrm{i}Z_1^2 \int \frac{\mathrm{d}q^4}{(2\pi)^4}\, v_{\boldsymbol{q}}\, D_{p-q} \times \left[(1+\chi_q\, v_{\mathrm{q}}) - 2\,\mathrm{i}Z_1 \int \frac{\mathrm{d}^4 q_1}{(2\pi)^4}\, D_{p-q_1}\, D_{p-q+q_1}\, Y_{q,-q_1}\, v_{\boldsymbol{q}_1} v_{\boldsymbol{q}-\boldsymbol{q}_1} \right] \tag{2.56}$$

where χ_q and Y_{q_1,q_2} represent the *exact* density correlation functions of the interacting FEG, as obtained from equations (2.23) and (2.24), respectively.

If the probe particle is an ion ($M \gg 1$), the propagator D_p and the energy p^0 entering equation (2.56) can be safely approximated by the non-interacting propagator D_p^0 and energy $\omega_{\boldsymbol{p}}$. Furthermore, recoil can be neglected, and one easily finds

$$D^0_{p-q} = -\frac{1}{q^0 - \boldsymbol{q}\cdot\boldsymbol{v} - \mathrm{i}\,\eta}. \tag{2.57}$$

In order to exploit the symmetry properties of Y_{q_1,q_2} it is useful to rewrite the retarded probe-particle propagator in terms of its Feynman version as follows:

$$D^0_{p-q} = -\frac{1}{q^0 - \boldsymbol{q}\cdot\boldsymbol{v} + \mathrm{i}\,\eta_q} - 2\,\mathrm{i}\,\pi\,\delta(q^0 - \boldsymbol{q}\cdot\boldsymbol{v})\,\Theta(q^0). \tag{2.58}$$

Introducing equation (2.58) into equation (2.56) and noting that the time-ordered density correlation functions χ_q and Y_{q_1,q_2} are invariant under the changes $(q^0 \to -q^0)$ and $(q_1^0 \to -q_1^0, q_2^0 \to -q_2^0)$, respectively, some work of rearrangement leads us to the following expression:

$$\Sigma_{\boldsymbol{p},\omega_{\boldsymbol{p}}} = 2\pi Z_1^2 \int \frac{\mathrm{d}q^4}{(2\pi)^4} v_{\boldsymbol{q}} \left[(1 + \chi_q \, v_{\boldsymbol{q}}) - \frac{4}{3}\pi Z_1 \right.$$
$$\left. \times \int \frac{\mathrm{d}^4 q_1}{(2\pi)^4} Y_{q,-q_1} \, v_{\boldsymbol{q}_1} v_{\boldsymbol{q}-\boldsymbol{q}_1} \, \delta\left(q_1^0 - \boldsymbol{q}_1 \cdot \boldsymbol{v}\right) \right] \delta(q^0 - \boldsymbol{q} \cdot \boldsymbol{v}) \, \Theta(q^0). \qquad (2.59)$$

Within RPA, the density correlation functions χ_q and Y_{q_1,q_2} are those given by equations (2.25) and (2.26). Beyond RPA, they are obtained from equations (2.29) and (2.30) in terms of the non-interacting density correlation functions (χ_q^0 and Y_{q_1,q_2}^0) and the effective e–e interaction of equation (2.28). Hence, introduction of equation (2.59) into equation (2.55) yields the following expression for the decay rate:

$$\tau^{-1} = 4\pi \, Z_1^2 \int \frac{\mathrm{d}q^4}{(2\pi)^4} \, v_{\boldsymbol{q}} \, \delta(q^0 - \boldsymbol{q} \cdot \boldsymbol{v}) \, \Theta(q^0)$$
$$\times \left[-\mathrm{Im}\, K_q + \frac{4}{3} \pi \, Z_1 \int \frac{\mathrm{d}^4 q_1}{(2\pi)^4} \, \mathrm{Im} \left(\tilde{K}_q \, Y_{q,-q_1}^0 \, \tilde{K}_{q_1} \, \tilde{K}_{q-q_1} \right) \right.$$
$$\left. \times \, v_{\boldsymbol{q}_1} v_{\boldsymbol{q}-\boldsymbol{q}_1} \, \delta\left(q_1^0 - \boldsymbol{q}_1 \cdot \boldsymbol{v}\right) \right] \qquad (2.60)$$

where K_q and $\tilde{K}_q$ represent the inverse dielectric functions of equations (2.27) and (2.32), with the density correlation function χ_q being given in both cases by equation (2.29).

The equivalence of equations (2.45) and (2.60) follows from the expansion of the imaginary part of $\tilde{K}_q \, Y_{q,-q_1}^0 \, \tilde{K}_{q_1} \tilde{K}_{q-q_1}$ in equation (2.60) and the use of equation (2.44) and the symmetry properties of Y_{q_1,q_2}^0 and $\tilde{K}(q^0, \boldsymbol{q})$. However, while (2.45) has been derived by only introducing self-energy and vertex insertions that can be described with the use of a static local-field factor, we have now demonstrated that either equation (2.45) or equation (2.60) can be used with inclusion of many-body dynamic local-field corrections.

Finally, we note that although both equation (2.45) (derived from equation (2.17)) and equation (2.60) (derived from equation (2.55)) represent the total decay rate, the integrands of these integral representations do not necessarily coincide with the probability $(\gamma_q^{\text{single}} + \gamma_q^{\text{double}} + \cdots)$ for the probe particle to transfer four-momentum q to the FEG. Consequently, the stopping power of the FEG for the probe particle (see equation (2.46)) cannot be obtained by simply inserting q^0/v inside the integral of equation (2.45) or equation (2.60), and the knowledge of the self-energy alone is not, therefore, sufficient to calculate the stopping power.

2.3. Quadratic response

In reference [10] the stopping power of a heavy probe particle was calculated using the framework of quadratic response theory. It was found that

$$-\frac{\mathrm{d}E}{\mathrm{d}x} = 4\pi Z_1^2 \int \frac{\mathrm{d}^4 q}{(2\pi)^4} \, q^0 \, v_{\boldsymbol{q}} \, \delta(q^0 - \boldsymbol{q} \cdot \boldsymbol{v}) \, \Theta(q^0)$$
$$\times \left[-\mathrm{Im}\, K_q^R + 2\pi Z_1 \int \frac{\mathrm{d}^4 q_1}{(2\pi)^4} \, \mathrm{Im} \left(\tilde{K}_q^R \, Y_{q,-q_1}^{R,0} \, \tilde{K}_{q_1}^R \, \tilde{K}_{q-q_1}^R \right) \right.$$
$$\left. \times \, v_{\boldsymbol{q}_1} \, v_{\boldsymbol{q}-\boldsymbol{q}_1} \, \delta\left(q_1^0 - \boldsymbol{q}_1 \cdot \boldsymbol{v}\right) \right] \qquad (2.61)$$

where K_q^R, $\tilde{K}_q^R$ and Y_{q_1,q_2}^R represent the retarded counterparts of K_q, $\tilde{K}_q$ and Y_{q_1,q_2}, respectively.

In order to compare this result with the one quoted in section 2 we must recall the relationship between the time-ordered and retarded functions.

In our case of interest, differences in the inverse dielectric functions arises from differences in the FEG density correlation function χ^0. We have

$$\operatorname{Re}\chi_q^{R,0} = \operatorname{Re}\chi_q^0 \tag{2.62}$$

$$\operatorname{Im}\chi_q^{R,0} = \operatorname{sgn}(q^0)\ \operatorname{Im}\chi_q^0. \tag{2.63}$$

The relationship between Y_{q_1,q_2} and Y_{q_1,q_2}^R is best analysed using their spectral representations. Y_{q_1,q_2}^R has the same structure as equation (2.24), with η_q replaced by a positive η [7]. This property leads to the following relations between imaginary and real part of the time-ordered and retarded $Y_{q1,q2}^0$ functions:

$$\operatorname{Re}\left(Y_{q_1,q_2}^0 - Y_{q_1,q_2}^{R,0}\right) = J_{-q_2,q_3} + J_{-q_3,q_2} \tag{2.64}$$

and

$$\operatorname{Im} Y_{q_1,q_2}^{R,0} = \tfrac{1}{2}\left[\operatorname{sgn}\left(q_1^0\right)\ H_{q_1,-q_2} - \operatorname{sgn}\left(q_2^0\right)\ H_{-q_2,q_1} - \operatorname{sgn}\left(q_3^0\right)\ H_{-q_3,q_2} + (q_2 \to q_3)\right]. \tag{2.65}$$

After some work of rearrangement and taking into account the symmetry properties of the functions involved, we find that equation (2.61) coincides exactly with equation (2.46). As in the case of the decay rate of equation (2.60), we find that both equations (2.46) and (2.61) can be used with inclusion of many-body dynamic local-field corrections. We also note that within RPA both equations (2.46) and (2.61) reduce to the result derived in references [5]–[9][2].

3. Conclusions

We have developed various many-body theoretical approaches to the quadratic decay rate and energy loss of charged particles moving in an electron gas, with inclusion of short-range XC effects.

We have carried out a perturbative formulation of the scattering matrix to derive general expressions for both the total decay rate and the average energy loss of arbitrary moving charged particles that are distinguishable from the electrons in the Fermi gas. Simplified expressions for these quantities have been obtained in the case of heavy probe particles ($M \gg 1$). The total decay rate of heavy particles has then been rederived from the knowledge of the probe-particle self-energy and it has been proved that the stopping power of the heavy particle agrees with the result deduced using quadratic response theory. Comparison of the different formalisms for a heavy particle suggests that our results in the scattering formalism can be used with full inclusion of many-body dynamic local-field corrections.

It has also been shown that while the first-order contributions to the energy loss may be obtained from the total decay rate by simply inserting the energy transfer inside the integrand of this quantity, this procedure cannot be generalized to the description of the second-order energy loss. Since response theory is only valid for heavy particles, this implies that the stopping power of light particles must be calculated using scattering theory.

[2] In reference [9], the difference between the real parts of Y_{q_1,q_2}^0 and $Y_{q_1,q_2}^{R,0}$ (see equation (2.64)) was overlooked. As a result, the energy loss of equation (2.61) was found, within RPA, to be equivalent to that of equation (2.46), but with no inclusion of the term $f_5(q, q_1)$. This term is now found when equation (2.64) is taken into account.

Acknowledgments

The authors acknowledge partial support by the University of the Basque Country, the Basque Hezkuntza, Unibertsitate eta Ikerketa Saila and the Spanish Ministerio de Educación y Cultura.

References

[1] Echenique P M, Flores F and Ritchie R H 1990 *Solid State Phys.* **43** 229
[2] Andersen L H, Hvelplund P, Knudsen H, Moller S P, Pedersen J O P, Uggerhoj E, Elsener K and Morenzoni K 1989 *Phys. Rev. Lett.* **62** 1731
[3] Medenwaldt R, Moller S P, Uggerhoj E, Worm T, Hvelplund P, Knudsen H, Elsener K and Morenzoni E 1991 *Nucl. Instrum. Methods* B **58** 1
Medenwaldt R, Moller S P, Uggerhoj E, Worm T, Hvelplund P, Knudsen H, Elsener K and Morenzoni E 1991 *Phys. Lett.* A **155** 155
[4] Moller S, Uggerhoj E, Bluhme H, Knudsen H, Mikkelsen U, Paludan K and Moernzoni E 1997 *Nucl. Instrum. Methods* B **122** 162
Moller S, Uggerhoj E, Bluhme H, Knudsen H, Mikkelsen U, Paludan K and Moernzoni E 1997 *Phys. Rev.* A **56** 2930
[5] Sung C C and Ritchie R H 1983 *Phys. Rev.* A **28** 674
[6] Hu C D and Zaremba E 1988 *Phys. Rev.* B **37** 9268
[7] Esbensen H and Sigmund P 1990 *Ann. Phys., NY* **201** 152
[8] Pitarke J M, Ritchie R H and Echenique P M 1993 *Nucl. Instrum. Methods* B **79** 209
Pitarke J M, Ritchie R H, Echenique P M and Zaremba E 1993 *Europhys. Lett.* **24** 613
[9] Pitarke J M, Ritchie R H and Echenique P M 1995 *Phys. Rev.* B **52** 13883
[10] del Río Gaztelurrutia T and Pitarke J M 2000 *Phys. Rev.* B **62** 6862
[11] Fetter A L and Walecka J D 1971 *Quantum Theory of Many-Particle Systems* (New York: McGraw-Hill)
[12] Singwi K S and Tosi M P 1981 *Solid State Phys.* **36** 177
[13] Hubbard J 1957 *Proc. R. Soc.* A **240** 539
Hubbard J 1957 *Proc. R. Soc.* A **243** 336
[14] Sayasov Y S 1997 *J. Plasma Phys.* **57** 373
Tao Z C and Kalman G 1991 *Phys. Rev.* A **43** 973
[15] Kleinman L 1968 *Phys. Rev.* **172** 383
[16] Hedin L and Lundqvist B I 1971 *J. Phys. C: Solid State* **4** 2064